



Published in final edited form as:

*J Magn Magn Mater.* 2009 May ; 321(10): 1529–1532. doi:10.1016/j.jmmm.2009.02.080.

## Nanoscale assembly of amine functionalized colloidal iron oxide

K. C. Barick<sup>a</sup>, M. Aslam<sup>b</sup>, Pottumarthi V. Prasad<sup>c</sup>, Vinayak P. Dravid<sup>d,e,\*</sup>, and Dhirendra Bahadur<sup>a,f,\*</sup>

<sup>a</sup>Department of Metallurgical Engineering and Materials Science, Indian Institute of Technology Bombay, Mumbai 400076, India

<sup>b</sup>Department of Physics, Indian Institute of Technology Bombay, Mumbai 400076, India

<sup>c</sup>Department of Radiology, Evanston Northwestern Healthcare, Evanston, IL 60201, USA

<sup>d</sup>Department of Materials Science and Engineering, Northwestern University, Evanston, IL 60208, USA

<sup>e</sup>International Institute for Nanotechnology, Northwestern University, Evanston, IL 60208, USA

<sup>f</sup>Centre for Research in Nanotechnology and Science, Indian Institute of Technology Bombay, Mumbai 400076, India

### Abstract

We demonstrate a single-step facile approach for highly water stable assembly of amine-functionalized Fe<sub>3</sub>O<sub>4</sub> nanoparticles using thermal decomposition of Fe-chloride precursors in ethylene glycol medium in the presence of ethylenediamine. The average size of nanoassemblies is 40±1 nm, wherein the individual nanoparticles are about 6 nm. Amine functionalized properties are evident from FTIR, thermal and elemental analysis. The saturation magnetization and spin-echo  $r_2$  of the nanoassemblies were measured to be 64.3 emu/g and 314.6 mM<sup>-1</sup>s<sup>-1</sup>, respectively. The higher value of relaxivity ratio ( $r_2/r_1=143$ ) indicates that nanoassemblies are a promising high efficiency T2 contrast agent platform.

### Keywords

Nanoparticles; Nanoassemblies; MR contrast agent; Surface functionalization; Iron oxide

---

Magnetic resonance imaging (MRI) is a powerful clinical tool for the non-invasive diagnosis and post-therapy assessment of variety of diseases. The MRI technique relies upon the relaxation of water protons which depends on the magnetic field, pulse sequence, heterogeneous distribution and surrounding environment of water in the organism [1,2]. The interpretation of the resulting MR image helps demarcate and identify most of the tissues. The contrast can be improved by using positive or negative contrast enhancers [3]; negative contrast agents induce a large shortening of the transverse relaxation time (T2) leading to a darkening of MR images, wherein the close contact of water molecules with positive contrast agent is reflected by a brightness which echoes the shortening of longitudinal relaxation time (T1).

---

\*Corresponding Address: E-mail: dhiren@iitb.ac.in, Fax: +91-22-25723480; Tel: +91-22-25767632 (Prof. D. Bahadur), E-mail: v-dravid@northwestern.edu, Fax: +1-847-467-6573; Tel: +1-847-467-1363 (Prof. Vinayak P. Dravid).

**Publisher's Disclaimer:** This is a PDF file of an unedited manuscript that has been accepted for publication. As a service to our customers we are providing this early version of the manuscript. The manuscript will undergo copyediting, typesetting, and review of the resulting proof before it is published in its final citable form. Please note that during the production process errors may be discovered which could affect the content, and all legal disclaimers that apply to the journal pertain.

Superparamagnetic iron oxide nanoparticles are the most promising T2 contrast agents for non-invasive in vivo monitoring of molecular and cellular events [4-6]. Most of the work in this area has been focused on multi-step surface functionalization of superparamagnetic iron oxide nanoparticles for MRI applications [5-8]. Recently, monodispersed magnetic nanoparticles nanoassemblies (MNNA) made up of numerous superparamagnetic nanoparticles are attracting considerable interest because of their potential applications in MRI; iron oxide core of individual superparamagnetic nanoparticles in the nanoassembly becomes more efficient at dephasing the spins of surrounding water protons and hence, enhances T2 relaxation time [9-11]. Of late, advances in chemical synthesis have enabled the preparation of high quality functionalized nanoassemblies of tunable (size and shape) nanoparticles. This can lead to artificially enhanced relaxation properties generated by the accumulative interparticle interaction. Thus, self-aggregation or self-assembly through spatial arrangement of nanoparticles as building blocks is the fundamental mechanism by which different nanoparticle assembly motifs or even closed packed ordered structures form in materials. The forces that controlled the assembly are determined by competing noncovalent intramolecular or intraparticle interactions such as electrostatic interaction [12], hydrogen bonding [13], van der Waals [14] and dipole-dipole interactions [15] etc. Thus, well-defined ordered structures obtained through the assembly of nanocrystalline building blocks provide new opportunities for optimizing, tuning and/or enhancing the properties and performance of the materials.

Here, we demonstrate an environmentally and economically preferable one-step green chemistry approach for synthesizing highly water-stable Fe<sub>3</sub>O<sub>4</sub> nano-colloidal assemblies with enhanced T2 contrast properties as compared to commercially available contrast agent. Specifically, superparamagnetic amine functionalized Fe<sub>3</sub>O<sub>4</sub> MNNA were produced by thermal decomposition of the Fe-chloride precursors in biocompatible ethylene glycol medium in the presence of ethylenediamine (EDA) molecules.

## Materials and methods

All chemicals are of analytical grade and used as received. In a typical synthesis of amine functionalized Fe<sub>3</sub>O<sub>4</sub> nanoassemblies, 1 g of Fe-chloride precursors (Fe<sup>2+</sup>/Fe<sup>3+</sup> = 1:2), sodium acetate (2 g) and ethylenediamine (7 ml) were added to ethylene glycol (30 ml), and stirred vigorously by a magnetic stirrer at 70°C to obtain a clear homogeneous golden yellow coloured mixture. This reaction mixture was transferred into a round bottom flask and temperature was slowly increased to 197°C under reflux, and reacted for another 6 h. The black coloured precipitates were obtained by cooling the reaction mixture to room temperature and then thoroughly rinsed with water to remove the solvent and by products. During each rinsing step, samples were separated from the supernatant using a permanent magnet.

X-ray diffraction (XRD) patterns were recorded on a Philips powder diffractometer PW3040/60 with Cu K<sub>α</sub> radiation. The electron micrographs were taken by Hitachi HF 2000 Transmission Electron Microscope (TEM) for particle size determination. The infrared spectra were recorded in the range 2000-400 cm<sup>-1</sup> on a Fourier Transform Infrared spectrometer (FTIR, Magna 550, Nicolet Instruments Corporation, USA). The thermogravimetric analysis (TGA) was performed by TA Instruments SDT Q600 analyzer. The elemental analysis was carried out by FLASH EA 1112 series CHNS (O) analyzer (Thermo Finnigan, Italy). The concentration of metal ions in the samples was obtained by ICP-AES (8440 Plasmalab, Labtam, Australia). The field dependence magnetization (M vs. H), and temperature dependence magnetization under zero-field cooled (ZFC) and field-cooled (FC) conditions in an applied field of 500 Oe were measured by Quantum Design PPMS. The Curie temperature (T<sub>C</sub>) was determined in an applied field of 100 Oe using Vibrating Sample Magnetometer (VSM, Lake Shore, Model-7410).

The T1 and T2 relaxation times (s) of the samples were measured for different concentrations of Fe<sub>3</sub>O<sub>4</sub> nanoassemblies using a 3T clinical MRI scanner (General Electric Healthcare, USA). The different concentration of amine functionalized Fe<sub>3</sub>O<sub>4</sub> samples were prepared by diluting them with milliQ water (Resistance 18.2 MΩ). T1-weighted images were obtained with a multiple inversion recovery SE sequence (TR 2200 ms; TI 2100 ms, 800 ms, 400 ms, 200 ms and 50 ms; matrix 512×512) and T2-weighted images were obtained with an FSE sequence. The  $r_1$  and  $r_2$  relaxivities (mM<sup>-1</sup> s<sup>-1</sup>) were calculated from the slope of the linear plots of 1/T1 and 1/T2 versus Fe ion concentrations.

## Results and discussion

The XRD patterns of amine functionalized Fe<sub>3</sub>O<sub>4</sub> MNNA samples (Fig. 1a) reveal single phase Fe<sub>3</sub>O<sub>4</sub> inverse spinel structure. The presence of sharp and intense peaks confirmed the formation of highly crystalline nanoparticles. Fig. 1b shows the TEM image of amine functionalized Fe<sub>3</sub>O<sub>4</sub> MNNA (Inset: Magnified TEM image of a single Fe<sub>3</sub>O<sub>4</sub> MNNA). The electron micrographs show that spherical nanoassemblies are well defined, discrete and porous in nature. Each 'nanosized sphere' of average size  $40 \pm 1$  nm is made up of three-dimensionally (3D) spatially connected nanoparticles of average diameter of about 6 nm. These fine nanoparticles are presumably assembled spontaneously into porous spherical superstructure to minimize their surface energy. The formation of such spherical nanoassemblies may be dependent on the collective behavior of nanoparticles and the intermolecular forces existing between them.

Fig. 2 shows the FTIR spectra of (a) ethylenediamine and (b) amine functionalized Fe<sub>3</sub>O<sub>4</sub> MNNA samples. The IR bands observed at around 588 cm<sup>-1</sup> can be ascribed to the Fe-O vibrational mode of Fe<sub>3</sub>O<sub>4</sub>. The vibrational modes attributed to the free amine group such as NH<sub>2</sub> scissoring at 1595 cm<sup>-1</sup>, C-N stretching at 1320 cm<sup>-1</sup> and NH wagging at 932 cm<sup>-1</sup> are clearly observed in the FTIR spectrum of amine functionalized Fe<sub>3</sub>O<sub>4</sub> nanoassemblies with a slight shift in their band positions.

Fig. 3 shows the TGA plot of amine functionalized Fe<sub>3</sub>O<sub>4</sub> MNNA samples. A weight loss of about 2.9 % below 230°C can be ascribed to the removal of diamine modified glycol molecules attached to the surface of Fe<sub>3</sub>O<sub>4</sub> MNNA and entrapped solvent from the porous net work of nanoassemblies. The weight loss of about 2.3% between 230-310 °C may be associated with the transformation of Fe<sub>3</sub>O<sub>4</sub> to  $\gamma$ -Fe<sub>2</sub>O<sub>3</sub> phase upon thermal treatment [16]. Further, CHN elemental analysis of Fe<sub>3</sub>O<sub>4</sub> MNNA clearly indicates the presence of organic components (3.011% C, 0.656% H and 0.63% N) on the samples. Thus, the FTIR, CHN and TGA results confirmed that Fe<sub>3</sub>O<sub>4</sub> nanoparticles (MNNA) have been functionalized with amine groups during the synthesis. These amine functionalized magnetic nanoassemblies were found to be highly stable in water. The 'colloidal' stability may be due to the formation of hydrogen bonds between the amine groups of functionalized magnetic nanoparticles and water.

Fig. 4 shows the M vs. H plot of amine functionalized Fe<sub>3</sub>O<sub>4</sub> MNNA at 5 and 300 K. At 300 K, samples exhibit superparamagnetic behavior without magnetic hysteresis and remanence where as ferrimagnetic behavior with a coercivity of about 100 Oe is observed at 5 K (Inset 'a' of Fig. 4). This transition from superparamagnetic behavior at high temperature to ferro or ferrimagnetic behavior below the so-called blocking temperature is typically observed in magnetic nanoparticles. The saturation magnetizations of amine functionalized Fe<sub>3</sub>O<sub>4</sub> samples were found to be 64.3 and 80.0 emu/g at 300 K and 5 K, respectively. The ZFC-FC plot (Inset 'b' of Fig. 4) shows that the blocking temperature ( $T_B$ ) of the MNNA is 130 K as one would expect for superparamagnetic nanoparticles. Further, the Curie temperature ( $T_C$ ) of MNNA was found to be 853 K, which is in agreement with that reported for Fe<sub>3</sub>O<sub>4</sub> whereas the  $T_C$  of

$\gamma$ -Fe<sub>2</sub>O<sub>3</sub> is around 918 K [17-19]. These results suggest that the phase formed is Fe<sub>3</sub>O<sub>4</sub> rather than  $\gamma$ -Fe<sub>2</sub>O<sub>3</sub>.

T1-weighted and T2-weighted phantom images of amine functionalized Fe<sub>3</sub>O<sub>4</sub> MNNA with different Fe ion concentrations are shown in Fig. 5. It has been observed that T1 relaxation time decreases with increasing the Fe concentration from 0.006 mM to 0.097 mM, while T2 relaxation time reduces accordingly. The  $r_1$  and  $r_2$  relaxivities of amine functionalized Fe<sub>3</sub>O<sub>4</sub> nanoassemblies in water were found to be 2.2 mM<sup>-1</sup> s<sup>-1</sup> and 314.6 mM<sup>-1</sup> s<sup>-1</sup>, respectively, and the relaxivity ratio,  $r_2/r_1$  is 143 which is much higher than that of commercial contrast agents such as Resovist (SH U 555 A), Feridex (AMI-25) and Supravist (SH U 555 C) measured at 3T [20] shown in Table 1. The higher the relaxivity ratio, the higher is the T2 effect and the signal decreases on T2-weighted images. Thus, the high value of relaxivity ratio of Fe<sub>3</sub>O<sub>4</sub> MNNA indicates that these nanoassemblies are promising candidate for high efficiency T2 contrast agents. Such a significant improvement in the T2 MR signal arises from the synergistic magnetism of multiple Fe<sub>3</sub>O<sub>4</sub> nanoparticles of the assemblies. Further, the nanoassemblies formed by clustering of nanoparticles decreases the surface of iron oxide in contact with the solvent and hence decrease in the T1 relaxivity. The enhancement of T2 relaxivity reflects the ability of magnetic nanoassemblies to distort the local magnetic field effectively.

## Conclusion

A new class of water-stable amine functionalized Fe<sub>3</sub>O<sub>4</sub> nanoassemblies has been synthesized by a simple and green approach; high temperature decomposition of Fe-chloride precursors carried out in a biocompatible ethylene glycol medium in the presence of ethylenediamine molecules. The size of nanoassemblies is about 40 ± 1 nm while that of the individual nanoparticles is about 6 nm. The high value of saturation magnetization and relaxivity ratio indicates that these nanoassemblies are very promising high efficiency T2 contrast agents. Further, these amine groups on Fe<sub>3</sub>O<sub>4</sub> MNNA surface can provide accessible surface for routine conjugation of biomolecules through the well-developed bioconjugation chemistry for a number of biomedical applications, such as magnetic biolabeling, efficient bioseparation and contrast enhancement for magnetic resonance imaging (MRI).

## Acknowledgments

The financial support by Nano initiative of DST, Govt. of India is gratefully acknowledged. This research is supported by NSF-MWN (Grant No. DMR-0603184)- DST (Indo-US project) and by the Center for Cancer Nanotechnology Excellence (CCNE) initiative of the National Institutes of Health's National Cancer Institute under Award U54CA119341 at Northwestern University. Any opinions, findings, and conclusions or recommendations expressed in this material are those of the author(s) and do not necessarily reflect those of the National Institutes of Health. K. C. Barick acknowledges AICTE, India for the award of National Doctoral Fellowship and NSF-MWN program for support for research at and visit to Northwestern University. Part of this work was performed in the EPIC/NIFTI facility of the NUANCE centre (supported by NSF-NSEC, NSFMRSEC, Keck Foundation, the State of Illinois, and Northwestern University) at Northwestern University.

## References

1. Bottrill M, Kwok L, Long NJ. Chem Soc Rev 2006;35:557. [PubMed: 16729149]
2. Prasad, Pottumarthi V. Am J Physiol Renal Physiol 2006;290:F958. [PubMed: 16601297]
3. Aime S, Botta M, Terreno E. Adv Inorg Chem 2005;57:173.
4. Lee JH, Huh YM, Jun YW, et al. Nature Medicine 2007;13:95.
5. Aslam M, Schultz EA, Sun T, et al. Crystal Growth & Design 2007;7:471. [PubMed: 19305647]
6. Sosnovik DE, Nahrendorf M, Weissleder R. Basic Res Cardiol 2008;103:122. [PubMed: 18324368]
7. Huh YM, Jun YW, Song HT, et al. J Am Chem Soc 2005;127:12387. [PubMed: 16131220]
8. Nitin N, LaConte LEW, Zurkiya O, et al. J Bio Inorg Chem 2004;9:706. [PubMed: 15232722]

9. Berret JF, Schonbeck N, Gazeau F, et al. *J Am Chem Soc* 2006;128:1755. [PubMed: 16448152]
10. Lee J, Lee Y, Youn JK, et al. *Small* 2008;4:143. [PubMed: 18189246]
11. Jun YW, Seo JW, Cheon J. *Accounts Chem Res* 2008;41:179.
12. Caruso F, Caruso R, Möhwald H. *Science* 1998;282:1111. [PubMed: 9804547]
13. Boal AK, Ilhan F, DeRouchey JE, et al. *Nature* 2000;404:746. [PubMed: 10783884]
14. Scholz SM, Vacassy R, Lemaire L, et al. *Appl Organomet Chem* 1998;12:327.
15. Sukhanova A, Baranov AV, Klinov D, et al. *Nanotechnol* 2006;17:4223.
16. Cornell, RM.; Schwertmann, U. *The Iron Oxides*. VCH; New York: 1996. p. 135
17. Barick KC, Bahadur D. *Bull Mater Sci* 2006;29:595.
18. Liu H, Jiang EY, Zheng RK, et al. *J Phys: Condens Matter* 2003;15:8003.
19. Ebisu T, Watanabe T. *Phys Rev D* 1987;36:3359.
20. Rohrer M, Bauer H, Mintorovitch J, et al. *Invest Radiol* 2005;40:715. [PubMed: 16230904]

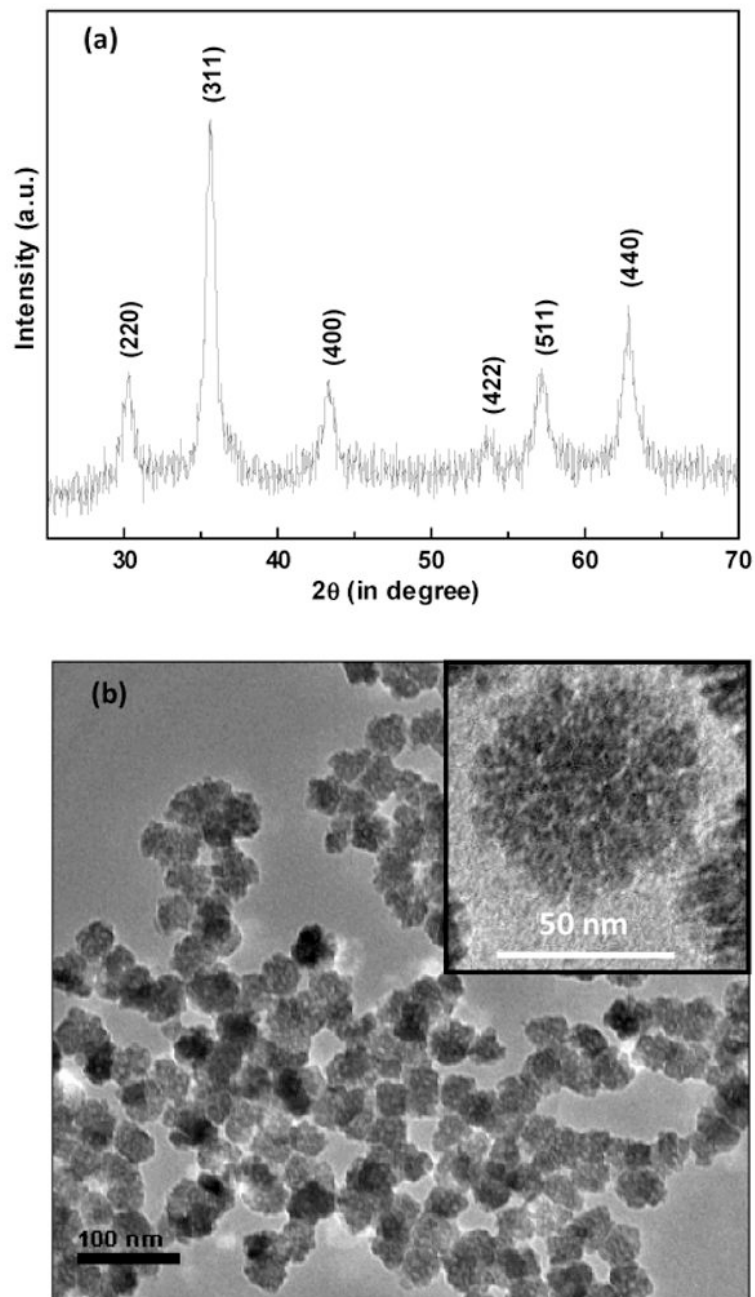


**Fig. 1.** (a) XRD patterns of amine functionalized  $\text{Fe}_3\text{O}_4$  MNNA samples (position and relative intensities of all diffraction peaks well matched with those from the Joint Committee on Powder Diffraction Standard (JCPDS) card 75-1609 of magnetite) and (b) TEM micrographs of amine functionalized  $\text{Fe}_3\text{O}_4$  MNNA samples (Inset: Magnified TEM image of a single  $\text{Fe}_3\text{O}_4$  MNNA).

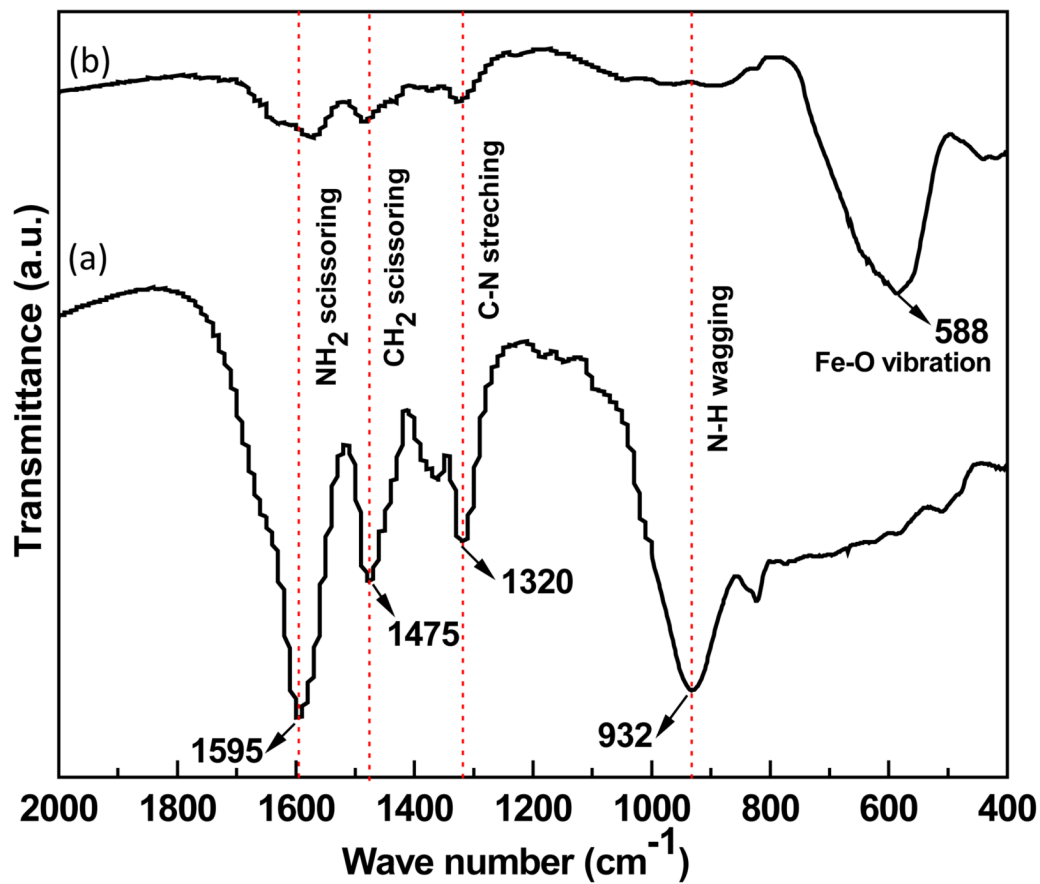
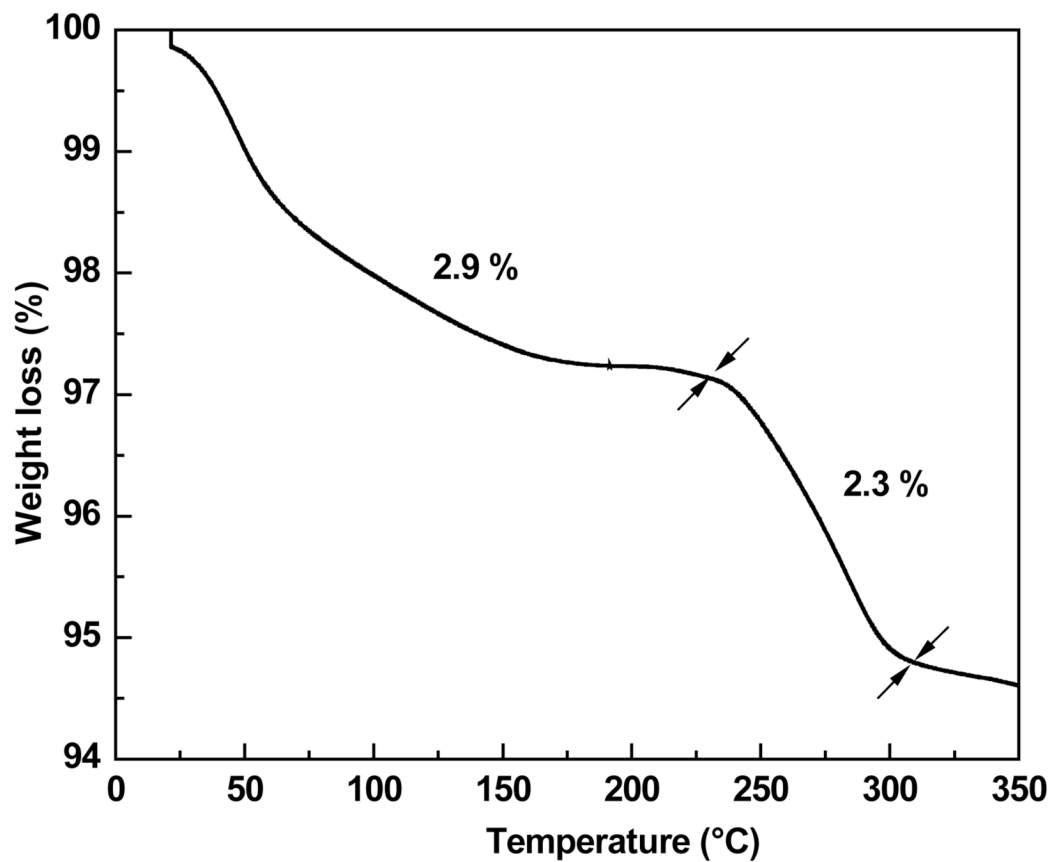


Fig. 2. FTIR spectra of (a) ethylenediamine and (b) amine functionalized Fe<sub>3</sub>O<sub>4</sub> MNNA samples.



**Fig. 3.** TGA plot of amine functionalized Fe<sub>3</sub>O<sub>4</sub> MNNA samples showing weight loss at different temperatures.



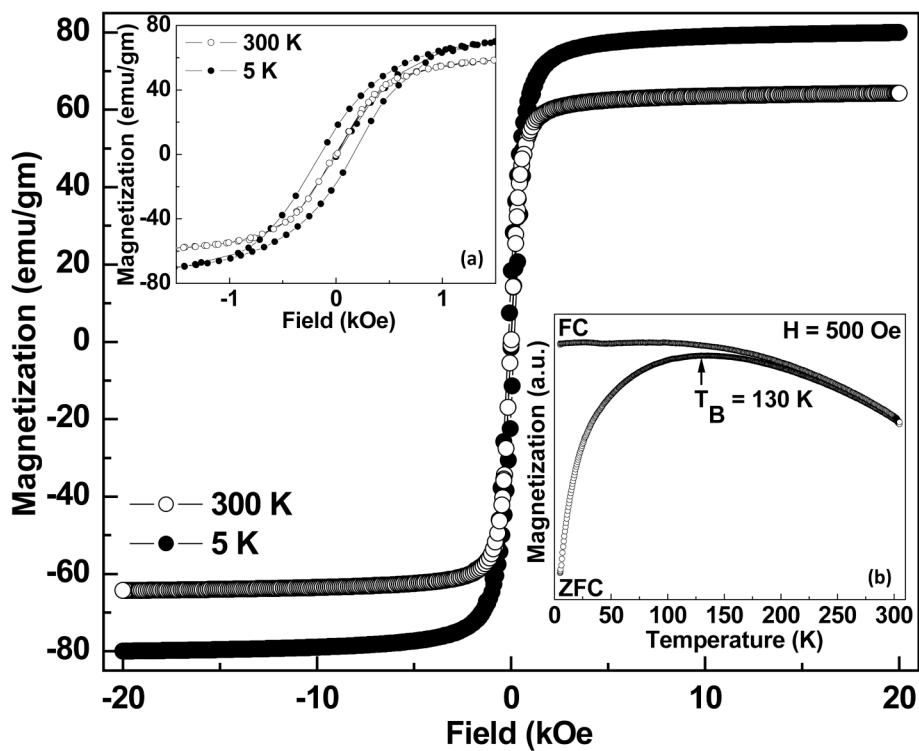
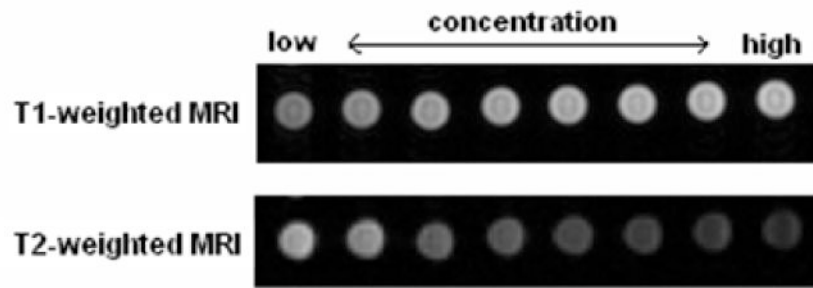


Fig. 4. M vs. H plot of amine functionalized  $\text{Fe}_3\text{O}_4$  MNNA. Inset: (a) its expanded M vs. H plot at low field region showing coercivity and (b) its ZFC-FC plot showing  $T_B = 130$  K.



**Fig. 5.** T1-weighted and T2-weighted phantom images of amine functionalized  $\text{Fe}_3\text{O}_4$  MNNA with different Fe ion concentrations (from left: 0.006, 0.012, 0.025, 0.032, 0.039, 0.052, 0.065, 0.097 mM).

**Table 1**

The  $r_1$  and  $r_2$  relaxivities and relaxivity ratio ( $r_2/r_1$ ) of  $\text{Fe}_3\text{O}_4$  MNNA and commercial contrast agents: Resovist (SH U 555 A), Feridex (AMI-25) and Supravist (SH U 555 C) measured at 3T [20].

Materials	Surface functionality	$r_1$ ( $\text{mM}^{-1}\text{s}^{-1}$ )	$r_2$ ( $\text{mM}^{-1}\text{s}^{-1}$ )	$r_2/r_1$
$\text{Fe}_3\text{O}_4$ MNNA	Amine functionalized $\text{Fe}_3\text{O}_4$ superparamagnetic nanoassemblies	2.2	314.6	143
Resovist (SH U 555 A)	Carboxydextran-coated superparamagnetic iron oxide	4.6	143	31.0
Feridex (AMI-25)	Dextran-coated superparamagnetic iron oxide	4.1	93	22.6
Supravist (SH U 555 C)	Carboxydextran-coated superparamagnetic iron oxide	7.3	57	7.8